



Hydrogen storage using heterocyclic compounds: The hydrogenation of 2-methylthiophene

H.Y. Zhao^{a,*}, S.T. Oyama^{a,*}, E.D. Naeemi^b

^a Environmental Catalysis and Materials Laboratory, Department of Chemical Engineering, Virginia Polytechnic Institute and State University, 140 Randolph Hall, Blacksburg, VA 24061, United States

^b Asemblon Inc., 15340 NE 92nd Street, Suite B, Redmond, WA 98052-3521, United States

ARTICLE INFO

Article history:

Available online 5 April 2009

Keywords:

Hydrogen storage
Hydrogenation
Alkyl substituted thiophenes
2-Methylthiophene
Sulfides
Phosphides
Noble metals
Bimetallics

ABSTRACT

Alkyl substituted thiophenes are promising candidates for hydrogen carriers, as their dehydrogenation reactions are known to occur under mild conditions. Four types of catalysts, including supported noble metals, bimetallic noble metals, transition metal phosphides and transition metal sulfides, have been investigated for 2-methylthiophene (2MT) hydrogenation and ring-opening. The major products were tetrahydro-2-methylthiophene (TH2MT), pentenes and pentane, with very little C₅-thiols observed. The selectivity towards the desired product TH2MT follows the order: noble metals > bimetallics > phosphides > sulfides. The best hydrogenation catalyst was 2% Pt/Al₂O₃ which exhibited relatively high reactivity and selectivity towards TH2MT at moderate temperatures. Temperature-programmed reaction (TPR) experiments revealed that pentanethiol became the major product, especially with HDS catalysts like CoMoS/Al₂O₃ and WP/SiO₂.

© 2009 Elsevier B.V. All rights reserved.

1. Introduction

Hydrogen has been suggested as an ecologically clean energy carrier because it does not produce air pollution or greenhouse gases. It can be produced by conventional or emerging membrane technology [1–3]. Hydrogen has almost three times the energy content of gasoline based on weight, but only about a quarter based on volume [4]. Lower-cost, lighter-weight and higher-density hydrogen storage is one of the key requirements for hydrogen energy use.

The US Department of Energy has set technology targets for hydrogen storage for 2010 and 2015. It is desired by 2010 to develop hydrogen storage systems achieving a gravimetric density of 2 kWh/kg (6 wt.%), a volumetric density of 1.5 kWh/L, and a cost of \$4/kWh, and by 2015, corresponding quantities of 3 kWh/kg (9 wt.%), 2.7 kWh/L, and \$2/kWh [4]. Currently four methods are being considered as promising candidates for hydrogen storage: compression and storage in conventional cylinders or cryogenic tanks, adsorption by metal hydrides, adsorption on high surface area materials, and chemical hydrogen storage (including off-board regeneration) [5].

High pressure storage needs high strength containers and has a limited volume capacity. A conventional steel hydrogen cylinder can hold only 1% by weight hydrogen and the boil-off of liquefied hydrogen requires venting, reduces driving range, and produces safety problems. Hydrogen liquefaction is also energy intensive at an expense of 30% of the heating value of hydrogen [6].

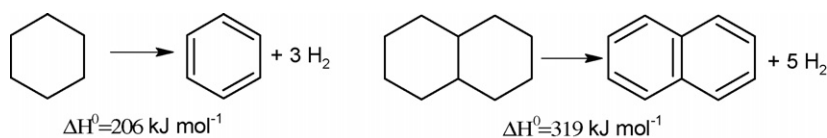
Metal hydrides are difficult to apply because they are too thermodynamically stable. This has two consequences. First, the hydrides have to be heated to an inconveniently high temperature to release hydrogen. Second, the heat of absorption is so high that a large amount of heat must be removed during the refueling process. In addition, the hydride systems contain strongly reducing agents which can react vigorously with air, and thus must be leak-free [7].

Adsorption of hydrogen onto high surface area materials, such as carbon nanotubes, has been studied extensively but also has barriers. These include the reproducibility of the synthesis of the material and the hydrogen storage performance [8].

Compared with the above methods, chemical hydrogen storage provides high gravimetric and volumetric hydrogen densities. Additionally, it has the advantage that hydrogen storage and transportation use conventional petrochemical substances [9].

Chemical hydrogen storage materials, also called organic chemical hydrides, employ hydrogenation–dehydrogenation of cyclic hydrocarbons or heteroaromatic compounds as a means to store and transport hydrogen. Aromatic compounds such as

* Corresponding author. Tel.: +1 540 231 5309; fax: +1 540 231 5022.
E-mail address: oyama@vt.edu (S.T. Oyama).



Scheme 1. Dehydrogenation of aromatic compounds.

benzene, toluene, and naphthalene can be easily hydrogenated by using appropriate metal catalysts under relatively mild conditions, e.g. about 100 °C and 2 MPa. However, the dehydrogenation of cyclic hydrocarbons is highly endothermic and the reaction is favored only at high temperatures (Scheme 1). Catalytic dehydrogenation under “liquid-film state” conditions has been reported [10–13], where the reactant is supplied as a liquid so that the surface of the catalyst is always wetted with a thin film. Equilibrium limits were surpassed because of the evaporation of the dehydrogenated reactants. Another method uses “wet-dry multiphase conditions” to take advantage of multiple phases to get over thermodynamic equilibrium limitations [14,15]. However, these two processes still require relatively high temperatures for vaporization of the volatile components of the process. An important need is also an effective separation of hydrogen from the mixtures to get a pure hydrogen product and to reuse the hydrogen carrier materials.

Heteroatom aromatic rings for H₂ storage were proposed recently because the addition of electron-donating groups favors H₂ release both thermodynamically and kinetically at moderate temperatures. In the case of indoline, dehydrogenation is possible at modest temperature (110 °C) [16]. Benzimidazolines, including N,N'-dimethyldihydrobenzimidazole, 1,3-dimethyl-2-phenylbenzimidazoline, and 1,3-dimethylbenzimidazoline, were studied with different palladium catalysts, and were found to release H₂ even at room temperature [17] (Scheme 2).

Hydrogen density is a very important factor in hydrogen storage. A lower weight of the organic framework needs to be developed while maintaining favorable thermochemical and kinetic parameters. Smaller molecules such as 4-aminopiperidine and piperidine-4-carboxamide are promising compounds for reversible hydrogen storage [18]. The dehydrogenation and hydrogenation of 4-aminopiperidine and piperidine-4-carboxamide occur easily at low temperatures without by-products, such as C–N cleavage and hydrogenolysis products. Density functional theory calculations suggest that dehydrogenation is greatly favored in five membered rings over six and by the incorporation of N atoms into the rings, either as ring substituents or as ring atoms, particularly in the 1 and 3 positions [19]. A number of heteroatom aromatic ligands have been used for reversible hydrogenation/dehydrogenation. For example, N-ethyl carbazole is hydrogenated with Pd at 72 atm and 160 °C and dehydrogenated with Ru at 50–197 °C [20] (Scheme 3).

The Asemlon hydrogen liquid storage system was proposed to utilize substituted thiophenes as carriers for storage, transport, and release of hydrogen [21]. This is based on the discovery that finely dispersed supported metal catalysts readily carry out the cyclization and dehydrogenation reaction of alkyl sulfides to

thiophene, at the same time releasing hydrogen. For example, for the case of 2-pentanethiol the reaction produces 2-methylthiophene (Scheme 4).

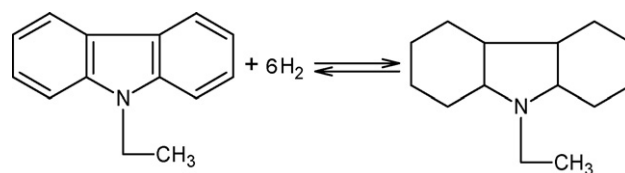
A method for catalytic hydrogenation of thiophenes needs to be established to use thiophenes as hydrogen carriers. The further cleavage of one of the C–S bonds, also called selective ring-opening (SRO), is more desirable because an additional mole of hydrogen can be carried than with the closed ring (Scheme 5).

In this work, 16 total catalysts are evaluated for the hydrogenation and ring-opening of 2MT, including supported noble metals, bimetallic noble metals, transition metal phosphides [22] and transition metal sulfides. Temperature-programmed desorption (TPD) of hydrogen provides insight into the relationship between hydrogen activation and the hydrogenation activities of the catalysts. Temperature-programmed reaction (TPR) is used to elucidate the reaction mechanism over the supported catalysts.

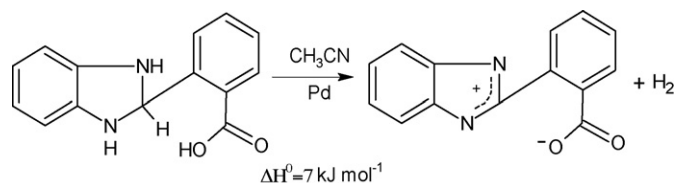
2. Experimental

2.1. Materials

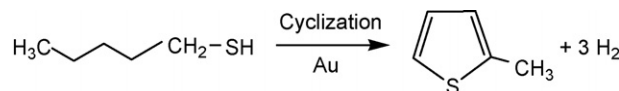
Commercial noble metal catalysts including Pt/Al₂O₃, Pd/Al₂O₃, and Ru/Al₂O₃ were provided by BASF Catalysts, Inc. Transition metal sulfides MoS/Al₂O₃, NiMoS/Al₂O₃, CoMoS/Al₂O₃ were obtained from Haldor Topsøe. Transition metal phosphides WP/SiO₂, Ni₂P/SiO₂, MoP/SiO₂ and bimetallics, PdPt/Al₂O₃ and PdRu/Al₂O₃ were synthesized. The support, fumed silica EH-5, was provided by Cabot Corp. The chemicals used in the synthesis of the catalysts were (NH₄)₆W₁₂O₃₉·xH₂O (Aldrich, 99%), Ni(NO₃)₂·6H₂O (Alfa Aesar, 99%), (NH₄)₆Mo₇O₂₄·4H₂O (Alfa Aesar, 99%), (NH₄)₂HPO₄ (Aldrich, 99%), Pd(NH₃)₄Cl₂·xH₂O (Alfa Aesar, 99.9%), Pt(NH₃)₄(NO₃)₂·xH₂O (Alfa Aesar, 99.9%) and RuCl₃·xH₂O (Alfa Aesar, 99.9%) were the precursors for the bimetallic catalysts. The chemicals used for the reactivity tests were 2-methylthiophene (Alfa Aesar, 98%) and n-nonane (Alfa Aesar, 99%). The gases employed were H₂ (Airco, Grade 5, 99.99%), He (Airco, Grade 5, 99.99%), CO (Linde Research Grade, 99.97%), 0.5% O₂/He (Airco, UHP Grade, 99.99%), O₂ (Airco, UHP Grade, 99.99%), 10% H₂S/H₂ (Airco, UHP Grade, 99.99%) and N₂ (Airco, Grade 5, 99.99%). Chemical standards for GC and mass spectrometry were tetrahydro-2-methylthiophene (TH2MT) (Alfa Aesar, 98%), pentanethiol (Alfa Aesar, 99%), pentane (Alfa Aesar, 99%), 1-pentene (Alfa Aesar, 99%), 2-pentene (Alfa Aesar, 99%).



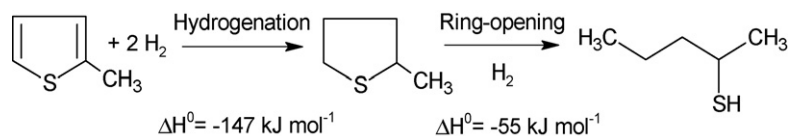
Scheme 3. Hydrogenation and dehydrogenation of N-ethyl carbazole.



Scheme 2. N,N'-dimethyldihydrobenzimidazole dehydrogenation.



Scheme 4. Dehydrogenation of pentanethiol.



Scheme 5. Hydrogenation and ring-opening of 2-methylthiophene.

2.2. Synthesis

WP/SiO₂ [23], Ni₂P/SiO₂ [24–26], MoP/SiO₂ [27,28], PdP/SiO₂ were prepared by TPR, following procedures reported previously [29,30]. Briefly, the synthesis of the catalysts involved two stages. First, solutions of the corresponding metal phosphate precursors were prepared by dissolving appropriate amounts of (NH₄)₆W₁₂O₃₉·xH₂O, Ni(NO₃)₂·6H₂O, (NH₄)₆Mo₇O₂₄·4H₂O, Pd(NH₃)₄Cl₂·xH₂O with ammonium phosphate in distilled water, and these solutions were used to impregnate silica by the incipient wetness method. The obtained samples were dried and calcined at 500 °C for 6 h, then ground with a mortar and pestle, pelletized with a press (Carver, Model C), and sieved to particles of 650–1180 μm diameter (16/20 mesh). Second, the solid phosphates were reduced to phosphides at 2 °C min⁻¹ in flowing H₂ [1000 cm³ (NTP) min⁻¹ g⁻¹]. Reduction temperatures were 577 °C for WP/SiO₂, 568 °C for Ni₂P/SiO₂, 494 °C for MoP/SiO₂, 350 °C for PdP/SiO₂. The samples were kept at the reduction temperature for 0.5 h, followed by cooling to RT under He flow [100 cm³ (NTP) min⁻¹], and then passivated at RT in a 0.5% O₂/He for 4 h. The Ni, Mo, W molar loading were all 1.6 mmol g⁻¹ (mmol per g of support), corresponding to a weight loading of Ni₂P of 7.9% with an initial Ni/P ratio of 1/2, MoP 12.8% with initial Mo/P ratio of 1, WP 19.9% with initial W/P ratio 1.

The bimetallic catalysts (1/4) PdPt/SiO₂, (4/1) PdPt/SiO₂ [31] and (4/1) PdRu/SiO₂ of total loading 2 wt.% with Pd/metal weight ratios (in parentheses) were synthesized by the incipient wetness method from the corresponding precursors dissolved in distilled water. After impregnation, the samples were dried in vacuum at 100 °C for 6 h, then calcined at 300 °C for 3 h [32].

2.3. Characterization

Irreversible CO uptake measurements were used to titrate the surface metal atoms and to provide an estimate of the active sites on the catalysts for the noble metals and the transition metal phosphides. Usually, 0.3 g of a passivated sample was loaded into a quartz reactor. Noble metal catalysts were reduced in H₂ at 325 °C for 2 h while passivated transition metal phosphides were reduced at 450 °C for 2 h. After cooling in He, pulses of CO in a He carrier at 43 μmol s⁻¹ [65 cm³ (NTP) min⁻¹] were injected at RT through a sampling valve, and the mass 28 (CO) signal was monitored with a mass spectrometer. CO uptake was calculated by measuring the decrease in the peak areas caused by adsorption in comparison with the area of a calibrated volume (19.5 μmol). Transition metal sulfides were characterized by the irreversible chemisorption of O₂ at dry-ice acetone temperature using the same techniques. Prior to the measurement the samples were sulfided in a flow of 10% H₂S/H₂ at 400 °C.

2.4. Reactivity studies

Hydrogenation activity was measured with a mixture containing 10 vol.% nonane and 90 vol.% 2MT at 2 MPa (300 psig) in a continuous-flow trickle bed reactor. Briefly, the testing unit consisted of three parallel reactors enclosed in heating ovens. The dimensions of the reactors were 1.5 cm i.d. × 25.5 cm long, and were generally loaded with 100 μmol active sites or 40 μmol for the samples with low uptakes. To start a reaction, catalysts were placed in the catalytic reactor and pretreated at the same conditions as used

for chemisorption. After pretreatment, the pressure was set to 2 MPa, a hydrogen flow rate of 150 cm³ NTP/min was started, and the liquid reactant was fed at a rate of 2.4 cm³/h. Reactivity testing was carried out as a function of temperature, which was started at the highest temperature 325 °C and was varied downwards and upwards with the initial temperature repeated at the end. Hydrotreating products were collected every few hours in sealed septum vials and quantified by a gas chromatograph (Hewlett-Packard, 5890A) equipped with a 0.32 mm i.d. × 50 m fused silica capillary column and a flame ionization detector. The reactants and products were identified by their retention time in comparison with commercially available standards and confirmed by gas chromatography–mass spectrometry (GC–MS) (Hewlett-Packard, 5890-5972A). Equilibrium calculations were carried out using the CHETAH program (ASTM International, West Conshohocken, PA).

2.5. TPD and TPR

The compounds Pt/Al₂O₃, PdPt/SiO₂, WP/SiO₂, and CoMoS/Al₂O₃ were the most active members of the four groups consisting of noble metals, bimetallics and transition metal phosphides and sulfides and were selected for further TPD and TPR tests. The TPD experiments were performed in a U-shaped quartz reactor connected to a mass spectrometer through a leak valve. The noble metal catalysts were pretreated in a flow of hydrogen at 325 °C for 2 h, and then cooled in hydrogen to 225 °C. After a He flush at the same temperature to remove the hydrogen background, the heating temperature program was started 5 °C/min to 450 °C. The mass 2 signal was monitored by MS. The sample was then cooled in helium to 225 °C and 2MT was introduced to the system in a helium carrier flow until saturation was reached. Then the system was heated to 550 °C at 5 °C/min in hydrogen. A total of 12 masses were monitored: 2, 4, 34, 42, 43, 55, 70 (pentene, or C₅H₁₀ fragment), 72 (pentane, or C₅H₁₂ fragment), 87, 97 (2MT), 102 (TH2MT), 104 (pentanethiol). The TPD and TPR were done with WP/SiO₂ and CoMoS/Al₂O₃ in a similar way except that they were pretreated at 450 °C in H₂ and 400 °C in H₂/H₂S, respectively.

3. Results and discussion

3.1. CO chemisorption and O₂ chemisorption

Uptakes of CO of the noble metal, bimetallic and transition metal phosphide catalysts are given in Table 1. Earlier studies have

Table 1
Summary of catalyst characterization by CO chemisorption.

Catalyst	CO uptake (μmol g ⁻¹)	Dispersion (%)	Particle size (nm)
0.5% Pd/Al ₂ O ₃	10	21	4
5% Pd/Al ₂ O ₃	120	25	4
0.5% Pt/Al ₂ O ₃	8	31	3
2% Pt/Al ₂ O ₃	44	42	2
0.5% Ru/Al ₂ O ₃	23	47	2
2% PdRu(4/1)/SiO ₂	140	77	1
2% PdPt(4/1)/SiO ₂	83	55	2
2% PdPt(1/4)/SiO ₂	99	84	1
Ni ₂ P/SiO ₂	95	8	11
MoP/SiO ₂	200	18	5
WP/SiO ₂	42	4	25
PdP/SiO ₂	74	56	2

Table 2Summary of catalyst characterization by O₂ chemisorption.

Catalyst	Composition	O ₂ uptake ($\mu\text{mol g}^{-1}$)	Dispersion (%)	Particle size (nm)
MoS/Al ₂ O ₃ (TK-Mo)	Mo 2–4.7%	58	55–23	2–4
NiMoS/Al ₂ O ₃ (TK-NiMo1)	Ni 0.8–2.4%; Mo 7–13%	54	17–9	5–10
NiMoS/Al ₂ O ₃ , AlPO ₄ (TK-NiMo2)	Ni 1.6–3.9%; Mo 8–12%, Al ₂ O ₃ 68–80%, AlPO ₄ 5–11%	68	12–7	9–13
CoMoS/Al ₂ O ₃ (TK-CoMo)	Co 2.4–4.7%; Mo 12–16%, support: 70–80%	100	12–8	7–11

shown that uptakes of the SiO₂ and Al₂O₃ supports were negligible [29,33–35]. The CO chemisorption uptakes of the different samples varied in a wide range from 8 to 200 $\mu\text{mol/g}$. It was found that for noble metals, higher loadings samples gave larger CO chemisorption uptakes but the average particle sizes (2–4 nm) did not vary appreciably. Bimetallic noble metal alloys were highly dispersed on the silica support surface and the particle sizes were small (1–2 nm). Among the phosphides the order of dispersion was WP/SiO₂ < Ni₂P/SiO₂ < MoP/SiO₂. For transition metal sulfides dispersion was approximated based on the O₂ chemisorption uptakes (Table 2). It was found that higher metal loadings gave

lower dispersion, although the total number of active sites increased with the metal loading, which is reasonable.

Assuming that each active site adsorbs one CO molecule or one oxygen atom, the number of active sites in the catalysts followed the order: sulfides > phosphides ~ bimetallics > noble metals.

3.2. Reactivity

A model feed containing 10 vol.% nonane and 90 vol.% 2MT was used to test the HDS and hydrogenation (HYD) activities of the 16 different catalysts. All the catalysts showed expected responses to

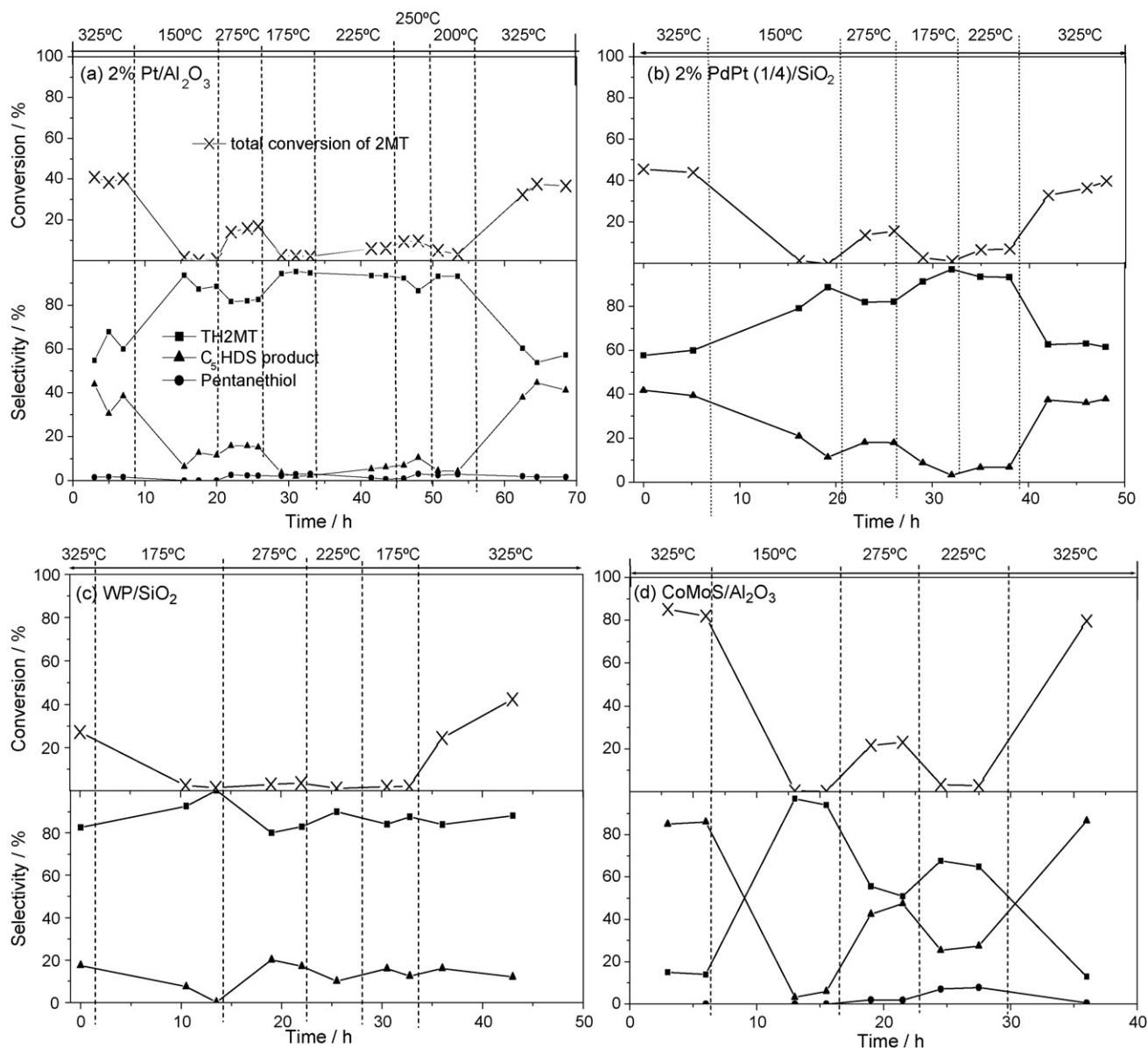


Fig. 1. Catalytic activity as a function of temperature. (a) 2% Pt/Al₂O₃, (b) 2% PdPt (1/4)/SiO₂, (c) WP/SiO₂ and (d) CoMoS/Al₂O₃.

temperature with higher conversions at higher temperatures and reasonable stability over the time course of the reactions. The major products were TH2MT, pentenes and pentane, but C₅-thiols could barely be observed. For convenience, all of the HDS products will be referred to as C₅ HDS products. Fig. 1 gives the conversion and selectivity of the four most active catalysts 2% Pt/Al₂O₃, 2% PdPt (1/4)/SiO₂, WP/SiO₂, CoMoS/Al₂O₃ out of the four groups of catalysts.

Fig. 2 summarizes reactivity results for all catalysts, presented as the total turnover frequency (TOF) for the 2MT reaction, the TOF of formation of TH2MT, the conversion of 2MT, and the selectivity to TH2MT. Fig. 2a shows that activities of the catalysts expressed as turnover frequency for the 2MT reaction follow the trend: noble metals > sulfides > bimetallics > phosphides. Fig. 2c shows that in terms of total conversion, the order is different, sulfides > phosphides ≈ noble metals > bimetallics. Fig. 2c also shows that TH2MT is the major hydrogenation product, followed by the HDS products, pentane and pentene. Very little pentanethiol was ever observed with all the catalysts, indicating that once this ring-opening reaction occurred, the thiols underwent desulfurization.

Fig. 2d shows the selectivity towards the desired product TH2MT. The order was noble metals > bimetallics > phosphides > sulfides. The order of selectivity towards TH2MT was opposite the order of the number of active sites of the catalysts, which indicates that active sites of the catalysts titrated by CO or O₂ chemisorption grossly favor HDS more than the hydrogenation product TH2MT. The most active catalysts were the sulfides with up to 80% conversion but with low selectivity to TH2MT of around 10% (Fig. 2a and d). This is expected, as these commercial sulfides are optimized for HDS. The noble metals (Pt and Pd) had conversion of 10–20% at lower temperatures and selectivity of 80–90%. At higher temperatures the noble metals had conversion of 40–50% but selectivity of 50–60%. The transition metal phosphides had very low conversions around 5% at low temperature with selectivity of 70–90%. At higher temperature transition metal phosphides had a conversion of 10–30% with selectivity of 30–80%. For the bimetallics, the conversions were about 10–15% at lower temperature with selectivity of 90%, while at a high temperature the conversion increased to 40–50% while selectivity decreased to 60–80%.

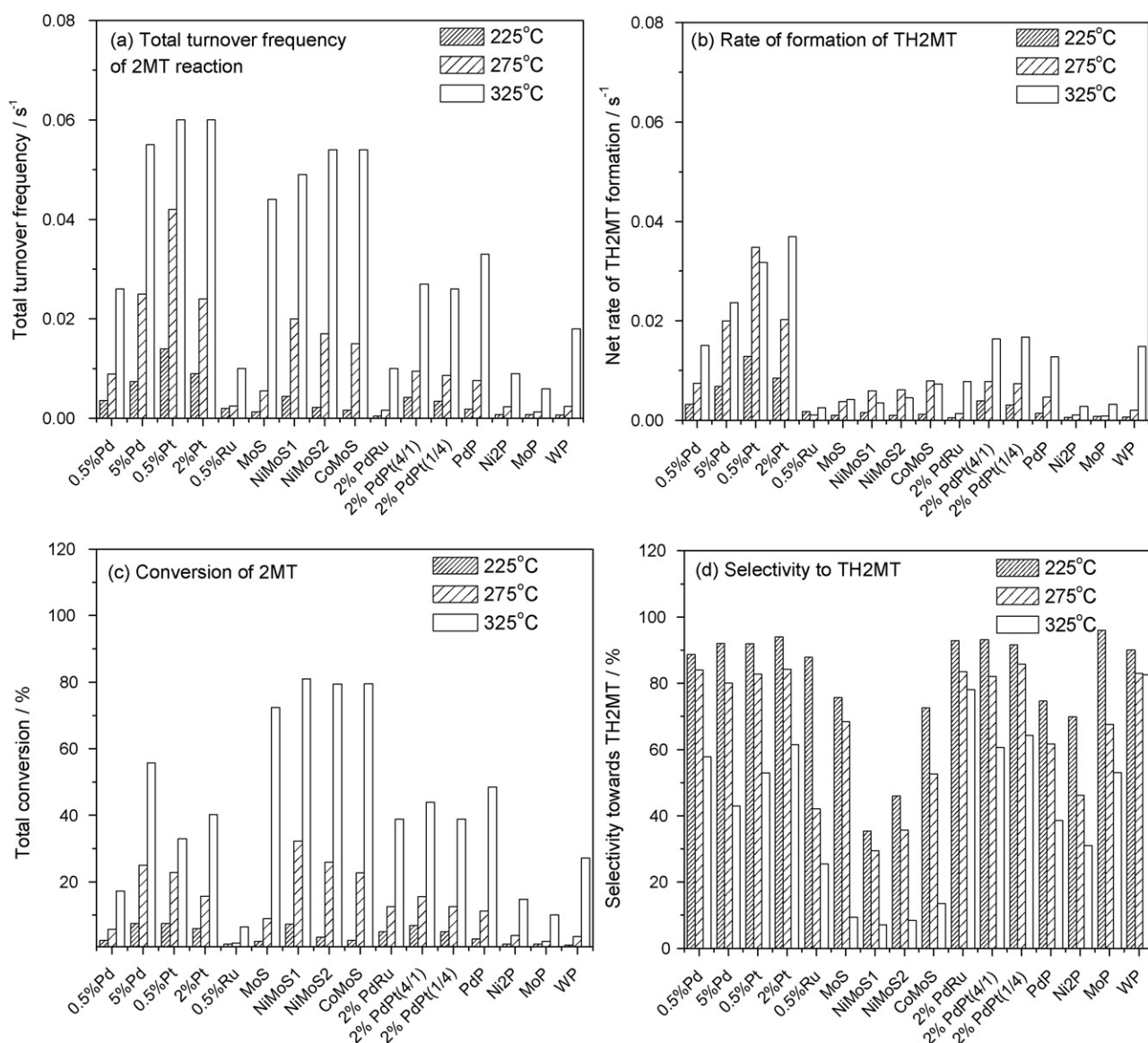


Fig. 2. Reactions of catalysts in the hydrogenations of 2-methylthiophene. (a) Turnover frequency of 2MT reaction, (b) rate of formation of TH2MT, (c) conversion of 2MT and (d) selectivity to TH2MT.

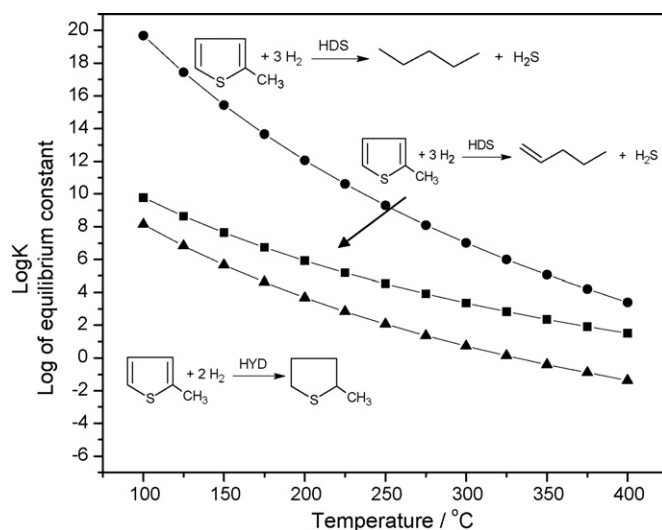


Fig. 3. Comparison of theoretical equilibrium constants for HDS and HYD.

Table 3
Comparison of active site determinations.

	2% PdPt(1/4)/SiO ₂	2% Pt/Al ₂ O ₃	CoMo/Al ₂ O ₃	WP/SiO ₂
H ₂ TPD desorption (μmol/g)	5	3	30	12
CO chemisorption (μmol/g)	44	99	– ^a	42
O ₂ chemisorption (μmol/g)	– ^a	– ^a	100	– ^a

^a Not measured.

Desulfurized products are favored at high temperatures and TH2MT is favored at low temperatures for all of the catalysts, which is consistent with theoretical equilibrium results: HDS was less favored at low temperatures (Fig. 3). As reaction temperature increased, the reactivity of 2MT increased while selectivity towards TH2MT decreased.

The results of the effect of pressure on the activity of 0.5% and 2% Pt/Al₂O₃ are summarized in Table 4. Comparison of the results on 0.5% and 2% Pt/Al₂O₃ of higher pressure (3.7 MPa, 550 psig) to

Table 4
Effect of pressure on the activity of 0.5% and 2% Pt/Al₂O₃.

Pressure (MPa, psig)	Catalyst	498 K		548 K		598 K	
		TOF (s ^{−1})	Selectivity (%)	TOF (s ^{−1})	Selectivity (%)	TOF (s ^{−1})	Selectivity (%)
2.0, 300	0.5% Pt/Al ₂ O ₃	0.01	92	0.04	83	0.06	53
	2% Pt/Al ₂ O ₃	0.009	94	0.02	84	0.06	60
3.7, 550	0.5% Pt/Al ₂ O ₃	0.01	96	0.03	84	0.05	50
	2% Pt/Al ₂ O ₃	0.006	95	0.02	87	0.04	59

Table 5
Product distribution for TPR of 2MT.

TPR of 2MT	2% PdPt(1/4)/SiO ₂		2% Pt/Al ₂ O ₃		CoMoS/Al ₂ O ₃		WP/SiO ₂	
	T _p (K)	μmol/g	T _p (K)	μmol/g	T _p (K)	μmol/g	T _p (K)	μmol/g
1-pentene (μmol/g)	590	0.06	670	0.3	560	0.3	560	0.1
Pentane (μmol/g)	– ^a	0	– ^a	0	550	0.1	– ^a	0
2MT (μmol/g)	– ^a	0	580	0.02	550	0.04	550	0.3
TH2MT (μmol/g)	– ^a	0	– ^a	0	640	0.04	640	0.03
Pentanethiol (μmol/g)	630	0.16	720	0.7	640	5	640	4.2
Total product (μmol/g)		0.2		1		5.6		4.6
Conversion (%)		100		98		99		99

^a Not observed.

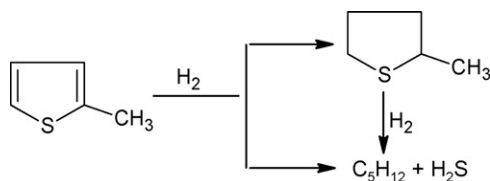
those obtained at standard conditions (20 MPa, 300 psig) shows that the selectivity for hydrogenation of 2-MT was slightly increased at lower temperatures (225 and 275 °C). However, at higher temperature (325 °C) the pressure change almost did not make a difference for the selectivity towards hydrogenation. The pressure did not show an obvious impact on the TOF either. Therefore, the activity studies for all the other catalysts were carried out at the lower pressure of 300 psig.

Thiophene reactions have been studied extensively in the field of hydroprocessing, because they are models for desulfurization of sulfur-containing heterocycles in petroleum feedstocks. However, the goal in hydroprocessing is to remove the sulfur atom (for a recent review see [36]) and the hydrogenation and ring-opening reactions have been considered just intermediary steps in the overall process. Studies on hydrogenation of thiophenes in the gas phase with Mo and W sulfides promoted with Ni and Co indicate that hydrogenolysis is facile and the hydrogenated products are only formed in small amounts [37], as found here. At 240 °C and 2 MPa, the activities of metal sulfides for the formation of tetrahydrothiophene are in the order: Pd » Mo > Rh ≥ Ru > Re > W > Co > Ni [38]. The higher activity of the palladium catalyst compared to the other sulfide catalysts is likely due to the ease of PdS reduction, which favors the formation of metallic sites for hydrogenation.

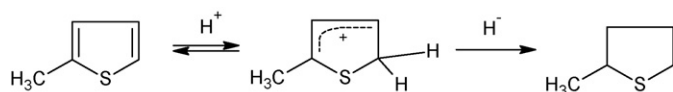
The methyl group at the α-carbon of 2MT increases the electron density on the aromatic ring and facilitates the activation of the ring. As a result, the rate of 2MT hydrogenation was reported to be almost an order of magnitude higher than that of thiophene hydrogenation [38]. The transformation of 2MT is believed to occur by a consecutive-parallel network on PdS because the selectivity to the hydrogenation product TH2MT and the hydrogenolysis product pentane are constant until the conversion reached 50% [39] (Scheme 6).

Supports with strong Brönsted acid surface sites like SiO₂, aluminosilicates, and zeolite HNaY showed much larger specific catalytic activity for the hydrogenation of 2MT than Al₂O₃, TiO₂, and carbon [40]. A commercial CoMo sulfide catalyst produced TH2MT and HDS products (pentenes and pentane) as the primary products [41]. The product 1-pentanethiol from the SRO of TH2MT was present in very small amounts.

Hydrogen dissociatively chemisorbs on the surface of sulfide catalysts and forms hydrogen atoms and ions [42]. 2MT is



Scheme 6. Hydrodesulfurization reaction mechanism for 2-methylthiophene.



Scheme 7. Hydrogenation mechanism for 2-methylthiophene.

protonated at the α -carbon and produces a thiophenium cation or a π -complex with coordinatively unsaturated surface cations to form the thiophenium cation. In the presence of a hydride ion donor, for example, a metal hydride, thiophene hydrogenation occurs by hydride transfer (Scheme 7) [38]. A similar 2MT hydrodesulfurization mechanism was proposed on metal sulfide catalysts [43]. The rate-determining step before the rupture of the C–S bond is the transfer of the first hydrogen to the adsorbed thiophenic compound.

The proton sites are very important for 2MT activation. Hydrides are thought to be a source of hydrogen for the hydrogenation and hydrogenolysis reactions. The TH2MT ring can be protonated and then made to undergo rupture through an elimination process to produce thiols.

Hydrogenation of aromatic and consecutive ring-opening can be carried out on certain noble metals. Pt, Pd, Ir, Ru and Rh supported on Al_2O_3 have been found active and selective for the

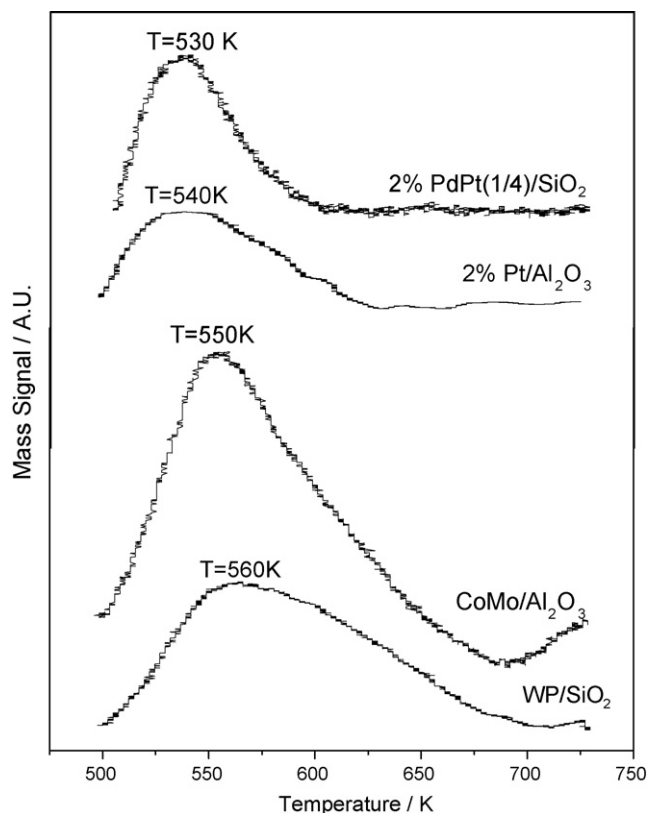


Fig. 4. TPD of H_2 profile.

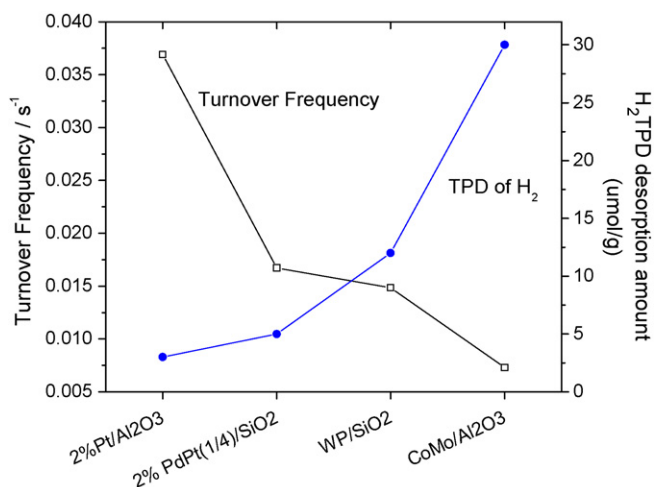


Fig. 5. Relation between turnover frequency and H_2 TPD desorption.

ring-opening of methylcyclopentane to the corresponding C_6 paraffins [44]. Ring-opening of naphthenes was seen to occur exclusively on the Brønsted acid sites of zeolites [45]. The number and strength distribution of Brønsted acid sites [46,47], the crystallite size [48], and the zeolite topology were all important parameters for the desired ring-opening products. When an effective acid functionality is combined with a high-activity hydrogenolysis metal, the bifunctional catalyst system will be greatly selective to the ring-opening products [49]. The commercial process for selective ring-opening involves such bifunctional catalysts. The acidic sites catalyze dehydrogenation, cracking, isomerization and dealkylation, while the metal sites carry out adsorption and desorption. Noble metals supported on acidic oxides are highly active catalysts for selective ring-opening [50]. All these transformations though occur on aromatics not containing heteroatoms, when heteroatoms like sulfur are present these molecules are removed by hydrogenolysis.

3.3. TPD and TPR

3.3.1. TPD of H_2

Based on their high reactivity and selectivity, 2% PdPt (1/4)/ SiO_2 , 2% Pt/ Al_2O_3 , CoMo/ Al_2O_3 , and WP/ SiO_2 were chosen for further study by TPD of H_2 and TPR of 2MT. The TPD experiments were started 498 K instead of room temperature so as to depopulate the low energy binding state of H_2 [51] and to only

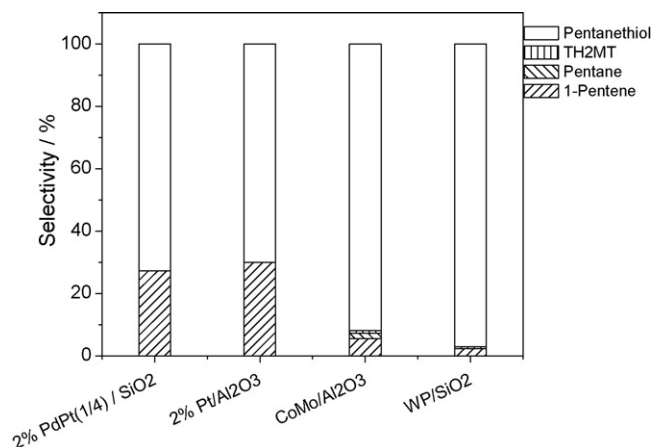


Fig. 6. Product Distribution for TPR of 2MT.

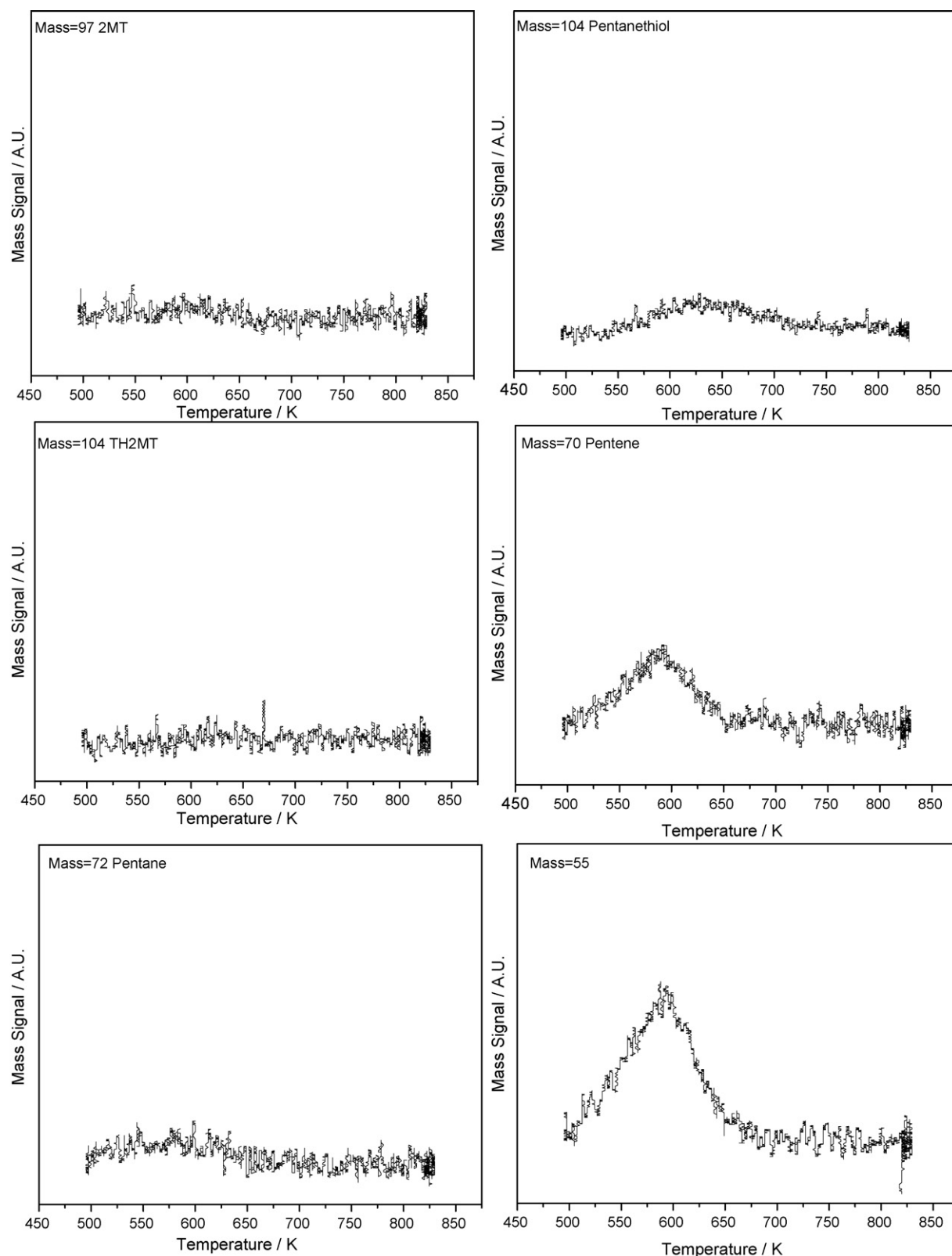


Fig. 7. TPR of 2MT on 2% PdPt/SiO₂ profiles.

examine the effective active sites in the range of temperatures used for the reaction of 2MT. Hydrogen desorption peak temperatures for 2% PdPt (1/4)/SiO₂, 2% Pt/Al₂O₃, and WP/SiO₂ were 530, 540, 550, 560 K, respectively (Fig. 4), which are comparable with results in the literature [52]. The order desorption of H₂ indicates that hydrogen is held slightly less strongly on the noble

metals than on the transition metal compounds, as expected. Hydrogen was also observed to desorb over a broad range of temperature on these four catalysts. The broad desorption spectra are possibly due to the site heterogeneity in the samples [53].

Table 3 compares the numbers of active sites measured by using different methods. The numbers measured by TPD of H₂ were much

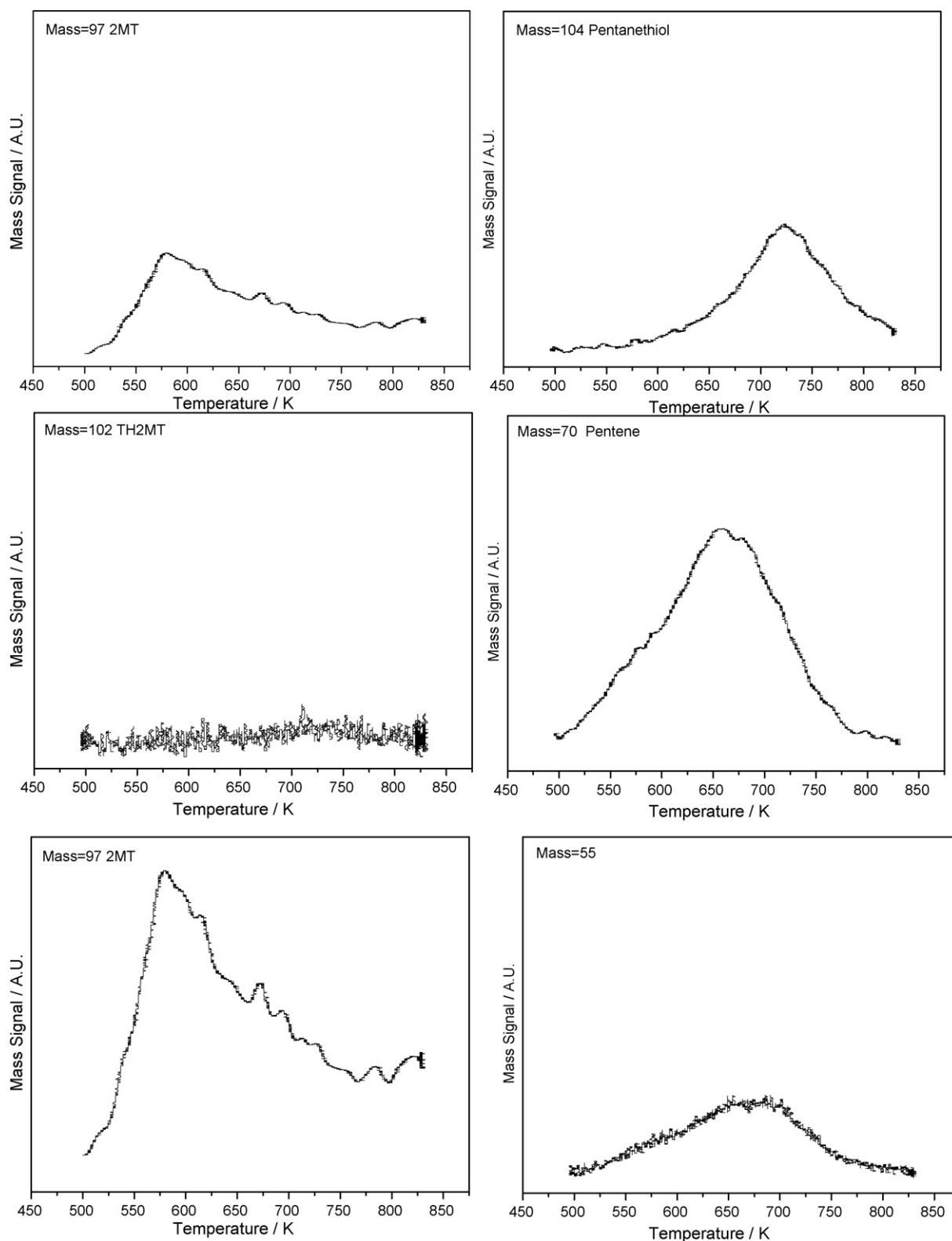


Fig. 8. TPR of 2MT on 2%Pt/Al₂O₃ profiles.

smaller than those titrated by CO or O₂ chemisorption. This is mainly because the lower energy binding states of hydrogen were excluded by the higher TPD starting temperature as mentioned above. H₂ TPD desorption amounts for these four catalysts followed a different order from the CO and O₂ chemisorption results.

It was found that the H₂ TPD desorption amount was inversely related to the rate of TH₂MT formation (Fig. 5). Since the H₂

desorption amount reflects the coverage of hydrogen at reaction conditions, this may indicate that hydrogen was consumed to a greater degree on the more active catalysts.

3.3.2. TPR of 2MT and H₂

Temperature programmed reduction experiments of 2MT were carried out with 2% PdPt (1/4)/SiO₂, 2% Pt/Al₂O₃, CoMo/Al₂O₃, and

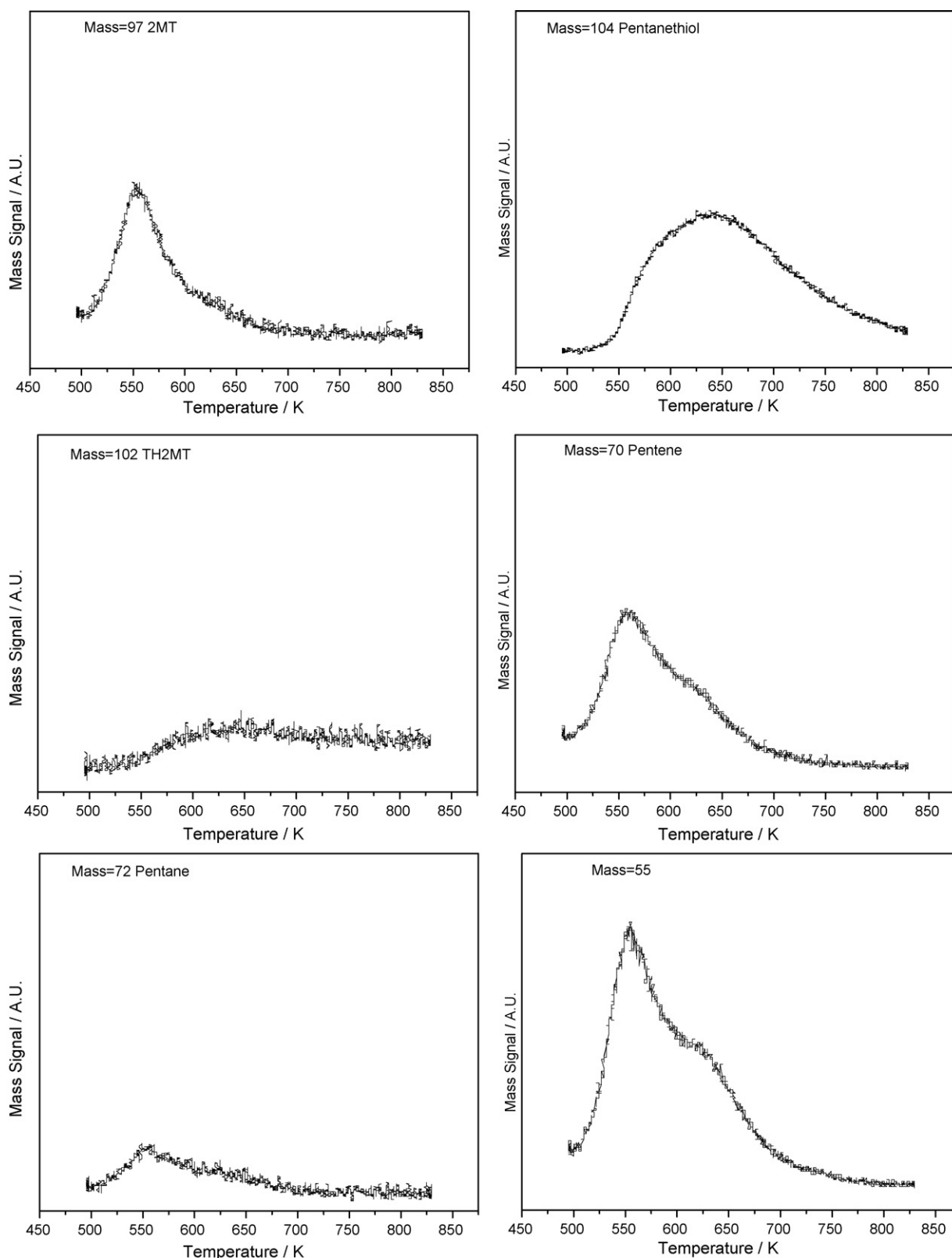


Fig. 9. TPR of 2MT on CoMo/Al₂O₃ profiles.

WP/SiO₂ (Figs. 7–10) and the desorption peaks were integrated to quantify the corresponding products (Table 5). The unreacted 2MT desorbed at a low temperature of around 550 K in a narrow peak but over 90% of the adsorbed 2MT reacted in the broad temperature range 498–823 K. The total amounts of 2MT adsorbed

on the catalysts followed the order: CoMo/Al₂O₃ > WP/SiO₂ > 2% Pt/Al₂O₃ > 2%PdPt (1/4)/SiO₂. This order matches the order found for the amount of desorbed H₂ in the TPD experiment, which indicates that the sites that are active for binding hydrogen are also active for 2MT hydrogenation. The major product in the TPR of 2MT

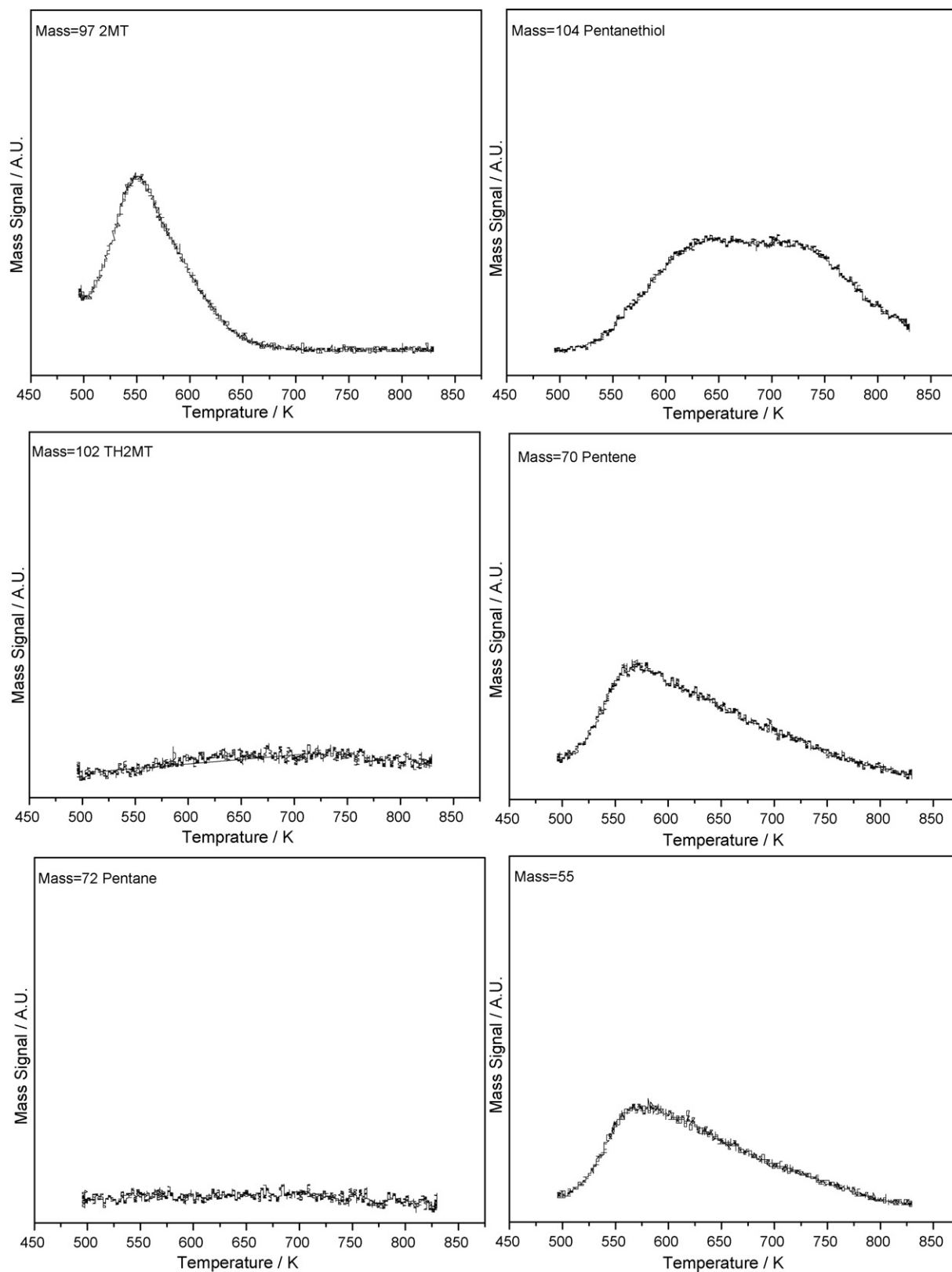
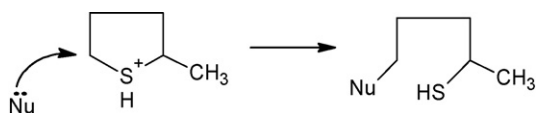
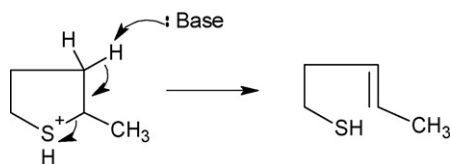


Fig. 10. TPR of 2MT on WP/SiO₂ profiles.

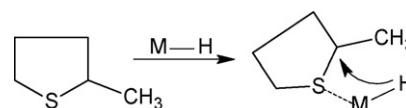


Scheme 8. S_N2 mechanism for 2MT ring-opening.

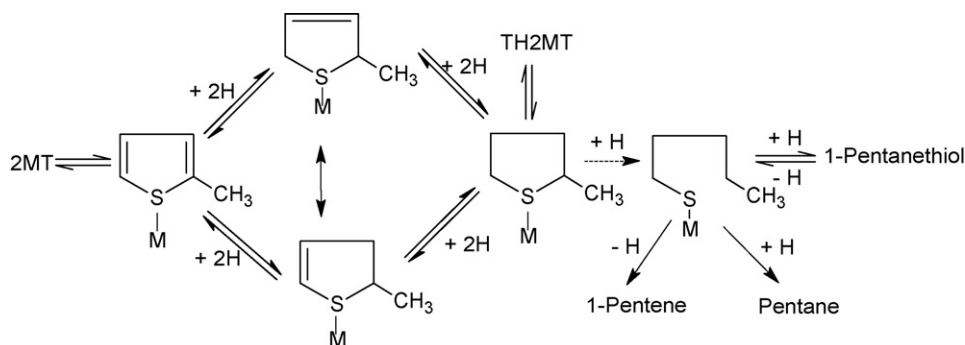
was the ring-opened product, pentanethiol, with some pentene also formed. The selectivities to TH2MT were no more than 6% and very little or no pentane was formed (Fig. 6). This is a reasonable finding. Generally the desulfurization of thiophenes involves two pathways [54]. One is the direct desulfurization pathway which in the case of 2MT gives pentenes or pentane. The other is the



Scheme 9. E2 mechanism for 2MT ring-opening.



Scheme 10. Metal hydride ring-opening of 2MT.



Scheme 11.

hydrogenation pathway which gives TH2MT followed by desulfurization of TH2MT. It has been reported that the reactivities of thiophenes and tetrahydrothiophenes are similar while those of thiols are about 15–40 times more reactive [55]. Thus, the formation of pentene or pentane and TH2MT is expected, not pentanethiol.

The products distribution of TPR of 2MT is shown in Fig. 6. Pentanethiol formed through the ring-opening of TH2MT was the major product. There are three pathways to ring-open TH2MT similar to the mechanisms of aromatic ring-opening, such as naphthalene [49]. Protonation of TH2MT followed by attack by a nucleophile will open the ring to form 2-pentanethiol because the S_N2 process favors the less hindered carbon (Scheme 8). On the other hand, attack by a base will tend to open the ring on the more substituted side by β elimination (Scheme 9). A third potential ring-opening pathway occurs on metal hydrides with Lewis acid properties. This will also favor attack on the more substituted side to form a 1-pentanethiolate intermediate (Scheme 10). In the TPR of 2MT, 2MT was adsorbed on the catalyst surface depleted of H_2 . It will be less likely for the adsorbed 2MT to be in the protonated form. Previous work has shown that supported metal catalysts which have one coordination vacancy can adsorb thiophene by the sulfur atom [56]. The preadsorbed 2MT would compete with hydrogen for sites on the surface [57]. Either carbon–sulfur scission or sulfur removal can be rate-controlling steps depending on the reaction conditions [57]. In this study sulfur removal is likely the rate controlling step because there TPR shows that more pentanethiol accumulates on the surface.

It was found that 2MT, pentanethiol and pentene desorbed at much higher temperatures on the 2% Pt/ Al_2O_3 surface compared with other catalysts. The interaction between 2% Pt/ Al_2O_3 and these species is stronger than with the other catalysts. Based on the results from the TPR of 2MT and evidence for the thiophene reaction mechanism [58], the following 2MT transformation network is proposed (Scheme 11).

4. Conclusions

Sixteen total catalysts were evaluated for the hydrogenation and ring-opening of 2MT, including supported noble metals, bimetallic noble metals, transition metal phosphides, and transi-

tion metal sulfides. The major products were TH2MT, pentenes and pentane, and C_5 -thiols could barely be observed. The selectivity towards the desired product TH2MT follows the order: noble metals > bimetallics > phosphides > sulfides. The order of selectivity towards TH2MT was opposite the order of the number of active sites of the catalysts, which indicates that the active sites of the catalysts titrated by CO or O_2 chemisorption favor HDS more than the hydrogenation product TH2MT.

TPD of hydrogen indicated that the H_2 desorption amount was inversely related to the rate of TH2MT formation. TPR showed that pentanethiol was the major product on the 2MT preadsorbed surface, especially on excellent HDS catalysts like CoMoS/ Al_2O_3 and WP/ SiO_2 .

References

- [1] Y. Gu, S.T. Oyama, *Adv. Mater.* 19 (2007) 1636.
- [2] Y. Gu, S.T. Oyama, *J. Membr. Sci.* 306 (2007) 216.
- [3] Y. Gu, P. Hacıoğlu, S.T. Oyama, *J. Membr. Sci.* 310 (2008) 28.
- [4] S. Satyapal, J. Petrovic, C. Read, G. Thomas, G. Ordaz, *Catal. Today* 120 (2007) 246–256.
- [5] Hydrogen storage roadmap, http://www1.eere.energy.gov/vehiclesandfuels/pdfs/program/hydrogen_storage_roadmap.pdf.
- [6] U. Bossel, B. Eliason, G. Taylor, <http://www.evworld.com/library/h2economyFinalReport.pdf>.
- [7] D.K. Ross, *Vacuum* 80 (2006) 1084–1089.
- [8] A. Anson, M. Benham, J. Jagiello, M.A. Callejas, A.M. Benito, W.K. Maser, A.Z. Uttel, P. Sudan, M.T. Martinez, *Nanotechnology* 15 (2004) 1503.
- [9] R.B. Biniwale, S. Rayalu, S. Devotta, M. Ichikawa, *Int. J. Hydrogen Energy* 33 (2008) 360–365.
- [10] N. Meng, S. Shinoda, Y. Saito, *Int. J. Hydrogen Energy* 22 (1997) 361–367.
- [11] S. Hodoshima, H. Arai, Y. Saito, *Int. J. Hydrogen Energy* 28 (2003) 197–204.
- [12] S. Hodoshima, H. Nagata, Y. Saito, *Appl. Catal. A: Gen.* 292 (2005) 90–96.
- [13] S. Hodoshima, S. Takaiwa, A. Shono, K. Satoh, Y. Saito, *Appl. Catal. A: Gen.* 283 (2005) 235–242.
- [14] N. Kariya, A. Fukuoka, T. Utagawa, M. Sakuramoto, Y. Goto, M. Ichikawa, *Appl. Catal. A: Gen.* 247 (2003) 247–259.
- [15] N. Kariya, A. Fukuoka, M. Ichikawa, *Appl. Catal. A: Gen.* 233 (2002) 91–102.
- [16] A. Moores, M. Poyatos, Y. Luo, R.H. Crabtree, *New J. Chem.* 30 (2006) 1675–1678.
- [17] D.E. Schwarz, T.M. Cameron, P.J. Hay, B.L. Scott, W. Tumas, D.L. Thorn, *Chem. Commun.* (2005) 5919–5921.
- [18] Y. Cui, S. Kwok, A. Bucholtz, B. Davis, R.A. Whitney, P.G. Jessop, *New J. Chem.* 32 (2008) 1027–1037.
- [19] E. Clot, O. Eisenstein, R.H. Crabtree, *Chem. Commun.* (2007) 2231–2233.
- [20] G.P. Pez, A.R. Scott, A.C. Cooper, H. Cheng, F.C. Wilhelm, A.H. Abdourazak, US Pat. 7,351,395, April 1, 2008, to Air Products and Chemicals, Inc.
- [21] B.D. Ratner, E.D. Naeemi, US Pat. 7,186,396, March 6, 2007, to Asemblon, Inc.
- [22] S.T. Oyama, *J. Catal.* 216 (2003) 343.
- [23] P. Clark, W. Li, S.T. Oyama, *J. Catal.* 200 (2001) 140.

- [24] S.T. Oyama, X. Wang, F. Requejo, T. Sato, Y. Yoshimura, J. Catal. 209 (2002) 1.
- [25] X. Wang, Y. Lee, S.T. Oyama, K. Bando, F.G. Requejo, J. Catal. 210 (2002) 207.
- [26] S.T. Oyama, X. Wang, Y.-K. Lee, W.-J. Chun, J. Catal. 221 (2004) 263.
- [27] W. Li, B. Dhandapani, S.T. Oyama, Chem. Lett. 3 (1998) 208.
- [28] S.T. Oyama, P. Clark, V.L.S. Teixeira da Silva, E.J. Lede, F.G. Requejo, J. Phys. Chem. B105 (2001) 4961.
- [29] P.A. Clark, X. Wang, S.T. Oyama, J. Catal. 207 (2002) 256.
- [30] X. Wang, P.A. Clark, S.T. Oyama, J. Catal. 208 (2002) 321.
- [31] K.K. Bando, T. Kawai, K. Asakura, T. Matsui, L.L. Bihan, H. Yasuda, Y. Yoshimura, S.T. Oyama, Catal. Today 111 (2006) 199.
- [32] K.K. Bando, T. Kawai, K. Asakura, T. Matsui, L.L. Bihan, H. Yasuda, Y. Yoshimura, S.T. Oyama, Catal. Today 111 (2006) 199–204.
- [33] P.A. Clark, X. Wang, P. Deck, J. Catal. 210 (2002) 216.
- [34] P.A. Clark, S.T. Oyama, J. Catal. 218 (2003) 78.
- [35] S.T. Oyama, Y.-K. Lee, J. Catal. 258 (2008) 393.
- [36] S.T. Oyama, T. Gott, H. Zhao, Y.-K. Lee, Catal. Today (2008), doi:10.1016/j.cattod.2008.09.019.
- [37] A.V. Mashkina, L.G. Salakhtueva, Chem. Heterocycl. Compd. 37 (2001) 546–549.
- [38] A.V. Mashkina, L.G. Sakhaltueva, Kinet. Catal. 43 (2002) 107–114.
- [39] A.A. Zirka, A.V. Mashkina, Kinet. Catal. 41 (2000) 388–393.
- [40] A.V. Mashkina, A.A. Zirka, Kinet. Catal. 41 (2000) 575–581.
- [41] D. Mey, S. Brunet, C. Canaff, F. Maugé, C. Bouchy, F. Diehl, J. Catal. 227 (2004) 436–447.
- [42] U. Roland, F. Roessner, Stud. Surf. Sci. Catal. 112 (1997) 191–200.
- [43] A. Daudin, A.F. Lamic, G. Pérot, S. Brunet, P. Raybaud, C. Bouchy, Catal. Today 130 (2008) 221–230.
- [44] F.G.J. Gault, Adv. Catal. 30 (1981) 1.
- [45] M.A. Arribas, P. Concepcion, A. Martinez, Appl. Catal. A 267 (2004) 111–119.
- [46] M.A. Arribas, J.J. Mahiques, A. Martinez, Stud. Surf. Sci. Catal. 135 (2001) 303.
- [47] M.A. Arribas, A. Martinez, Appl. Catal. A 230 (2002) 203.
- [48] M.A. Arribas, A. Martinez, G. Sastre, Stud. Surf. Sci. Catal. 142 (2002) 1015.
- [49] G.B. Mcvicker, M. Daage, M.S. Touvelle, C.W. Hudson, D.P. Klein, W.C. Baird Jr., B.R. Cook, J.G. Chen, S. Hantzer, D.E.W. Vaughan, E.S. Ellis, O.C. Feeley, J. Catal. 210 (2002) 137–148.
- [50] H. Du, C. Fairbridge, H. Yang, Z. Ring, Appl. Catal. A: Gen. 294 (2005) 1–21.
- [51] J.R. Anderson, K. Fogar, R.J. Breakspere, J. Catal. 57 (1979) 458.
- [52] P.G. Menon, G.F. Froment, Appl. Catal. 1 (1981) 31.
- [53] S. Smeds, T. Salmi, L.P. Lindfors, O. Krause, Appl. Catal. A: Gen. 144 (1996) 177–194.
- [54] H. Topsøe, B.S. Clausen, F.E. Massoth, Hydrotreating Catalysis, Catalysis-Science and Technology, Springer-Verlag, Berlin, 1996.
- [55] S. Kolboe, Can. J. Chem. 47 (1969) 352.
- [56] D.L. Sullivan, J.G. Ekerdt, J. Catal. 172 (1997) 64–75.
- [57] M. Neurock, R.A. Santan, J. Am. Chem. Soc. 116 (1994) 4427–4439.
- [58] D.L. Sullivan, J.G. Ekerdt, J. Catal. 178 (1998) 226–233.